Zentrum für Technomathematik

Fachbereich 3 – Mathematik und Informatik

Variational image restoration by means of wavelets: simultaneous decomposition,deblurring and denoising

I. Daubechies **G. Teschke**

Report 04–04

Berichte aus der Technomathematik

Report 04–04 **April 2004**

Variational image restoration by means of wavelets: simultaneous decomposition, deblurring and denoising

I. Daubechies* and G. Teschke†

March 29, 2004

Abstract

Inspired by papers of Vese–Osher [OV02] and Osher–Solé–Vese [OSV02] we present a wavelet–based treatment of variational problems arising in the field of image processing. In particular, we follow their approach and discuss a special class of variational functionals that induce a decomposition of images into oscillating and cartoon components and possibly an appropriate 'noise' component. In the setting of [OV02] and [OSV02], the cartoon component of an image is modeled by a BV function; the corresponding incorporation of BV penalty terms in the variational functional leads to PDE schemes that are numerically intensive. By replacing the BV penalty term by a $B_1^1(L_1)$ term (which amounts to a slightly stronger constraint on the minimizer), and writing the problem in a wavelet framework, we obtain elegant and numerically efficient schemes with results very similar to those obtained in [OV02] and [OSV02]. This approach allows us, moreover, to incorporate general bounded linear blur operators into the problem so that the minimization leads to a simultaneous decomposition, deblurring and denoising.

1 Introduction

One important problem in image processing is the restoration of the 'true' image from an observation. In almost all applications the observation is a noisy and blurred version of the true image. In principle, this problem can be understood as an inverse problem, i.e. one can attack the restoration problem by solving a related variational formulation.

In this paper we focus on a special class of variational problems which induce a decomposition of images in oscillating and cartoon components; the cartoon part is ideally piecewise smooth with possible abrupt edges and contours; the oscillation part on the other hand 'fills' in the smooth regions in the cartoon with texture - like features. Several authors, e.g. [OV02, OSV02], propose to model the cartoon component by the space BV which induces a penalty term that allows edges

*Princeton University, PACM, Washington Road, Princeton, NJ 08544-1000, USA
†University of Bremen, ZETEM, P.O.Box 330 440, 28334 Bremen, Germany

and contours in the reconstructed cartoon images. However, the minimization of variational problems of this type usually results in PDE based schemes which are numerically intensive.

The main goal of this paper is to provide a computationally thriftier algorithm by using a wavelet–based scheme that solves not the same but a very similar variational problem, in which the BV–constraint, which cannot easily be expressed in the wavelet domain, is replaced by a $B_1^1(L_1)$–term, i.e. a slightly stricter constraint (since $B_1^1(L_1) \subset BV$ in two dimensions). Moreover, we can allow the involvement of general linear bounded blur operators, which extends the range of application. By applying recent results, see [DDD03], we show convergence of the proposed scheme.

In order to give a brief description of the underlying variational problems, we recall the methods proposed in [OV02, OSV02]. They follow the idea of Y. Meyer [Mey02], proposed as an improvement on the total variation framework of L. Rudin, S. Osher and E. Fatemi [ROF92]. In principle, the models can be understood as a decomposition of an image f into $f = u + v$, where u represents the cartoon part and v the texture part. In the Vese–Osher model, see [OV02], the decomposition is induced by solving

$$\inf_{u,g_1,g_2} G_p(u, g_1, g_2) \ , \quad \text{where} \tag{1.1}$$

$$G_p(u, g_1, g_2) = \int_\Omega |\nabla u| + \lambda \|f - (u + \mathrm{div} g)\|^2_{L_2(\Omega)} + \mu \| |g| \|_{L_p(\Omega)} \ ,$$

with $f \in L_2(\Omega)$, $\Omega \subset \mathbb{R}^2$, and $v = \mathrm{div} g$. The first term is the total variation of u. If $u \in L_1$ and $|\nabla u|$ is a finite measure on Ω, then $u \in BV(\Omega)$. This space allows discontinuities, therefore edges and contours generally appear in u. The second term represents the restoration discrepancy; to penalize v, the third term approximates (by taking p finite) the norm of the space of oscillating functions introduced by Y. Meyer (with $p = \infty$) which is in some sense dual to $BV(\Omega)$. (For details we refer the reader to [Mey02].) Setting $p = 2$ and $g = \nabla P + Q$, where P is a single–valued function and Q is a divergence–free vector field, it is shown in [OSV02] that the v–penalty term can be expressed by

$$\| |g| \|_{L_2(\Omega)} = \left(\int_\Omega |\nabla (\Delta)^{-1} v|^2 \right)^{1/2} = \|v\|_{H^{-1}(\Omega)} \ .$$

(The H^{-1} calculus is allowed as long as we deal with oscillatory texture/noise components that have zero mean.) With these assumptions, the variational problem (1.1) simplifies to solving

$$\inf_{u,g_1,g_2} G_p(u, v) \ , \quad \text{where} \tag{1.2}$$

$$G_p(u, v) = \int_\Omega |\nabla u| + \lambda \|f - (u + v)\|^2_{L_2(\Omega)} + \mu \|v\|_{H^{-1}(\Omega)} \ .$$

In general, one drawback is that the minimization of (1.1) or (1.2) leads to numerically intensive schemes.

Instead of solving problem (1.2) by means of finite difference schemes, we propose a wavelet–based treatment. We are encouraged by the fact that elementary methods based on wavelet shrinkage solve similar extremal problems where

$BV(\Omega)$ is replaced by the Besov space $B_1^1(L_1(\Omega))$. Since $BV(\Omega)$ can not be simply described in terms of wavelet coefficients, it is not clear that $BV(\Omega)$ minimizers can be obtained in this way. Yet, it is shown in [CDPX99], exploiting $B_1^1(L_1(\Omega)) \subset BV(\Omega) \subset B_1^1(L_1(\Omega))-weak$, that methods using Haar systems provide near $BV(\Omega)$ minimizers. So far there exists no similar result for general (in particular smoother) wavelet systems. We shall nevertheless use wavelets that have more smoothness/vanishing moments than Haar wavelets, because we expect them to be better suited to the modeling of the smooth parts in the cartoon image. Though we may not obtain provable 'near–best–BV–minimizers', we hope to nevertheless not be 'too far off'. Limiting ourselves to the case $p = 2$, replacing $BV(\Omega)$ by $B_1^1(L_1(\Omega))$, and, moreover, extending the range of applicability by incorporating a bounded linear blur operator, we end up with the following variational problem

$$\inf_{u,v} \mathcal{F}_f(v,u) \ , \quad \text{where}$$

$$\mathcal{F}_f(v,u) = \|f - K(u+v)\|^2_{L_2(\Omega)} + \gamma\|v\|^2_{H^{-1}(\Omega)} + 2\alpha|u|_{B_1^1(L_1(\Omega))} \ .$$

This paper is organized as follows. In Section 2 we recall some basic facts on wavelets, in Section 3 the numerical scheme is developed and convergence is shown, in Section 4 we introduce some extra refinements on the scheme, and finally, in Section 5 we present some numerical results.

2 Preliminaries on wavelets

In this section, we briefly recall some facts on wavelets that are needed later on. Especially important for our approach are the smoothness characterization properties of wavelets: one can determine the membership of a function in many different smoothness functional spaces by examining the decay properties of its wavelets coefficients. For a comprehensive introduction and overview on this topic we would refer the reader to the abundant literature, see e.g. [Dau92, Dau93, CDF92, Dah96, DJP92, DJP88, FJ90, Tri78].

Suppose H is a Hilbert space. Let $\{V_j\}$ be a sequence of closed nested subspaces of H whose union is dense in H while their intersection is zero. In addition, V_0 is shift–invariant and $f \in V_j \leftrightarrow f(2^j\cdot) \in V_0$, so that the sequence $\{V_j\}$ forms a multi-resolution analysis. In many cases of practical relevance the spaces V_j are spanned by single scale bases $\Phi_j = \{\phi_{j,k} : k \in I_j\}$ which are uniformly stable. Successively updating a current approximation in V_j to a better one in V_{j+1} can be facilitated if stable bases $\Psi_j = \{\psi_{j,k} : k \in J_j\}$ for some complement W_j of V_j in V_{j+1} are available. Hence, any $f_n \in V_n$ has an alternative multi-scale representation $f_n = \sum_{k\in I_0} f_{0,k}\phi_{0,k} + \sum_{j=0}^{n}\sum_{k\in J_j} f_{j,k}\psi_{j,k}$. The essential constraint on the choice of W_j is that $\Psi = \bigcup_j \Psi_j$ forms a Riesz-basis of H, i.e. every $f \in H$ has a unique expansion

$$f = \sum_j \sum_{k\in J_j} \langle f, \tilde{\psi}_{j,k}\rangle \psi_{j,k} \ \text{ such that } \ \|f\|_H \sim \left(\sum_j \sum_{k\in J_j} |\langle f, \tilde{\psi}_{j,k}\rangle|^2\right)^{\frac{1}{2}} , \qquad (2.1)$$

where $\tilde{\Psi}$ forms a bi-orthogonal system and is in fact also a Riesz-basis for H, cp. [Dau92].

For our approch we assume that any function (image) $f \in L_2(I)$ can be extended periodically to all of $\mathbb{R}^2$. Here I is assumed to be the unit square $(0,1]^2 = \Omega$. Throughout this paper we only consider compactly supported tensor product wavelet systems (based on Daubechies' orthogonal wavelets, see [Dau93], or symmetric bi-orthogonal wavelets by Cohen, Daubechies, and Feauveau, see [CDF92]).

We are finally interested in characterizations of Besov spaces, see, e.g., [Tri78]. For $\beta > 0$ and $0 < p, q \leq \infty$ the Besov space $B_q^\beta(L_p(\Omega))$ of order β is the set of functions

$$B_q^\beta(L_p(\Omega)) = \{f \in L_p(\Omega) : \ |f|_{B_q^\beta(L_p(\Omega))} < \infty\} \ ,$$

where $|f|_{B_q^\beta(L_p(\Omega))} = \left(\int_0^\infty (t^{-\beta}\omega_l(f;t)_p)^q dt/t\right)^{1/q}$ and ω_l denotes the l-th modulus of smoothness, $l > \beta$. These spaces are endowed with the norm $\|f\|_{B_q^\beta(L_p(\Omega))} = \|f\|_{L_p(\Omega)} + |f|_{B_q^\beta(L_p(\Omega))}$. (For $p < 1$, this is not a norm, strictly speaking, and the Besov spaces are complete topological vector spaces but no longer Banach spaces, see [DeV98] for details, including the characterization of these spaces by wavelets.) What is important to us is that one can determine whether a function is in $B_q^\beta(L_p(\Omega))$ simply by examining its wavelet coefficients. The case $p = q$, on which we shall focus, is the easiest. Suppose that ϕ has R continuous derivatives and ψ has vanishing moments of order M. Then, as long as $\beta < \min(R, M)$, one has in, two dimensions, for all $f \in B_p^\beta(L_p(\Omega))$,

$$|f|_{B_p^\beta(L_p(\Omega))} \sim \left(\sum_\lambda 2^{|\lambda| s p} |f_\lambda|^p\right)^{1/p} \quad \text{with} \quad f_\lambda := \langle f, \tilde{\psi}_\lambda \rangle \text{ and } s = \beta + 1 - 2/p \ . \quad (2.2)$$

In what follows, we shall always use the equivalent weighted ℓ_p–norm of the $\{f_\lambda\}$ instead of the standard Besov norm; with a slight abuse of notation we shall continue to denote it by the same symbol, however. When $p = q = 2$, the space $B_2^\beta(L_2(\Omega))$ is the Bessel potential space $H^\beta(\Omega)$. In analogy with the special case of Bessel potential spaces $H^\beta(\Omega)$, the Besov space $B_p^\beta(L_p(\Omega))$ with $\beta < 0$ can be viewed as the dual space of $B_{p'}^{\beta'}(L_{p'}(\Omega))$, where $\beta' = -\beta$ and $1/p + 1/p' = 1$.

3 Image decomposition

As stated in Section 1, we aim to solve

$$\inf_{u,v} \mathcal{F}_f(v,u) \ , \quad \text{where} \quad (3.1)$$

$$\mathcal{F}_f(v,u) = \|f - K(u+v)\|_{L_2(\Omega)}^2 + \gamma \|v\|_{H^{-1}(\Omega)}^2 + 2\alpha |u|_{B_1^1(L_1(\Omega))} \ .$$

At first, we may observe the following

Lemma 3.1 *If the null–space $\mathcal{N}(K)$ of the operator K is trivial, then the variational problem* (3.1) *has a unique minimizer.*

This can be seen as follows:

$$\mathcal{F}_f(\mu(v,u)+(1-\mu)(v',u')) - \mu\mathcal{F}_f((v,u)) - (1-\mu)\mathcal{F}_f((v',u')) =$$

$$-\mu(1-\mu)\left(\|K(u-u'+v-v')\|^2_{L_2(\Omega)} + \gamma\|v-v'\|^2_{H^{-1}(\Omega)}\right)$$
$$+2\alpha\left(|\mu u+(1-\mu)u'|_{B^1_1(L_1(\Omega))} - \mu|u|_{B^1_1(L_1(\Omega))} - (1-\mu)|u'|_{B^1_1(L_1(\Omega))}\right) \quad (3.2)$$

with $0 < \mu < 1$. Since the Banach norm is convex the right hand side of (3.2) is non-positive, i.e. $\mathcal{F}_f$ is convex. Since $\mathcal{N}(K) = \{0\}$, the term $\|K(u-u'+v-v')\|$ can be zero only if $u-u'+v-v'=0$, moreover, $\|v-v'\|$ is zero only if $v-v'=0$. Hence, (3.2) is strictly convex. ■

In order to solve this problem by means of wavelets we have to switch to the sequence space formulation. When K is the identity operator the problem simplifies to

$$\inf_{u,v}\left\{\sum_{\lambda\in J}\left(|f_\lambda-(u_\lambda+v_\lambda)|^2+\gamma 2^{-2|\lambda|}|v_\lambda|^2+2\alpha|u_\lambda|\cdot 1_{\{\lambda\in J_{j_0}\}}\right)\right\}. \quad (3.3)$$

The minimization of (3.3) is straightforward, since it decouples into easy one–dimensional minimizations. This results in an explicit shrinkage scheme, presented also in [DT04]:

Proposition 3.1 *Let f be a given function. The functional* (3.3) *is minimized by the parametrized class of functions $\tilde{v}_{\gamma,\alpha}$ and $\tilde{u}_{\gamma,\alpha}$ given by the following non-linear filtering of the wavelet series of f:*

$$\tilde{v}_{\gamma,\alpha} = \sum_{\lambda\in J_{j_0}}(1+\gamma 2^{-2|\lambda|})^{-1}\left[f_\lambda - S_{\alpha(2^{2|\lambda|}+\gamma)/\gamma}(f_\lambda)\right]\psi_\lambda$$

and

$$\tilde{u}_{\gamma,\alpha} = \sum_{k\in I_{j_0}}\langle f,\tilde{\phi}_{j_0,k}\rangle\phi_{j_0,k} + \sum_{\lambda\in J_{j_0}} S_{\alpha(2^{2|\lambda|}+\gamma)/\gamma}(f_\lambda)\psi_\lambda\ ,$$

where S_t denotes the soft-shrinkage operator.

In the case where K is not the identity operator the minimization process results in a coupled system of nonlinear equations for the wavelet coefficients u_λ and v_λ, which it is not as straightforward to solve. To overcome this problem, we adapt an iterative approach. As in [DDD03] we derive the iterative algorithm from a sequence of so-called surrogate functionals that are each easy to minimize, and for which one hopes that the successive minimizers have the minimizing element of (3.1) as limit. However, contrary to [DDD03] our variational problem has mixed quadratic and non-quadratic penalties. This requires a slightly different use of surrogate functionals. In [DD03b, DD03a] a similar $u+v$ problem is solved by an approach that combines u and v into one vector–valued function (u,v). This leads to alternating iterations with respect to u and v simultaneously. It can be shown that the minimizers of the resulting alternating algorithm strongly converge to the desired unique solution, [DD03b].

We will follow a different approach here, in which we first solve the quadratic problem for v, and then construct an iteration scheme for u. To this end, we introduce the differential operator $T := (-\Delta)^{1/2}$. Setting $v = Tw$ the variational problem (3.1) reads as

$$\inf_{(u,w)} \mathcal{F}_f(w,u) \ , \quad \text{with} \tag{3.4}$$

$$\mathcal{F}_f(w,u) = \|f - K(u+Tw)\|^2_{L_2(\Omega)} + \gamma\|w\|^2_{L_2(\Omega)} + 2\alpha|u|_{B^1_1(L_1(\Omega))} \ .$$

Minimizing (3.4) with respect to w results in

$$\tilde{w}_\gamma(f,u) = (T^*K^*KT + \gamma)^{-1}T^*K^*(f - Ku)$$

or equivalently

$$\tilde{v}_\gamma(f,u) = T(T^*K^*KT + \gamma)^{-1}T^*K^*(f - Ku) \ .$$

Inserting this explicit expression for $\tilde{w}_\gamma(f,u)$ in (3.4) and defining

$$f_\gamma := T_\gamma f, \quad T^2_\gamma := Id - KT(T^*K^*KT + \gamma)^{-1}T^*K^* \ , \tag{3.5}$$

we obtain

$$\mathcal{F}_f(\tilde{w}_\gamma(f,u),u) = \|f_\gamma - T_\gamma Ku\|^2_{L_2(\Omega)} + 2\alpha|u|_{B^1_1(L_1(\Omega))} \ . \tag{3.6}$$

Thus, the remaining task is to solve

$$\inf_u \mathcal{F}_f(\tilde{w}_\gamma(f,u),u) \ , \quad \text{where} \tag{3.7}$$

$$\mathcal{F}_f(\tilde{w}_\gamma(f,u),u) = \|f_\gamma - T_\gamma Ku\|^2_{L_2(\Omega)} + 2\alpha|u|_{B^1_1(L_1(\Omega))} \ .$$

The corresponding variational equations in the sequence space representation are

$$\forall\lambda \ : \quad (K^*T^2_\gamma Ku)_\lambda - (K^*f_\gamma)_\lambda + \alpha\text{sign}(u_\lambda) = 0 \ .$$

This gives a coupled system of nonlinear quations for u_λ. For this reason we construct surrogate functionals that remove the influence of $K^*T^2_\gamma Ku$. First, we choose a constant C such that $\|K^*T^2_\gamma K\| < C$. Since $\|T_\gamma\| \le 1$, it suffices to require that $\|K^*K\| < C$. Then we define the functional

$$\Phi(u;a) := C\|u-a\|^2_{L_2(\Omega)} - \|T_\gamma K(u-a)\|^2_{L_2(\Omega)}$$

which depends on an auxiliary element $a \in L_2(\Omega)$. We observe that $\Phi(u,a)$ is strictly convex in u for any a. Since K can be rescaled, we limit our analysis without loss of generality to the case $C = 1$. We finally add $\Phi(u;a)$ to $\mathcal{F}_f(\tilde{w}_\gamma(f,u),u)$ and obtain the following surrogate functional

$$\begin{aligned}
\mathcal{F}^{sur}_f(\tilde{w}_\gamma(f,a),u;a) &= \mathcal{F}_f(\tilde{w}_\gamma(f,u),u) + \Phi(u;a) \\
&= \sum_\lambda \{u^2_\lambda - 2u_\lambda(a + K^*T^2_\gamma(f - Ka))_\lambda + 2\alpha|u_\lambda|\} \\
&\qquad + \|f_\gamma\|^2_{L_2(\Omega)} + \|a\|^2_{L_2(\Omega)} - \|T_\gamma Ka\|^2_{L_2(\Omega)} \ .
\end{aligned} \tag{3.8}$$

The advantage of minimizing (3.8) is that the variational equations for u_λ decouple. The summands of (3.8) are differentiable in u_λ expect at the point of non-differentiability. The variational equations for each λ are now given by

$$u_\lambda + \alpha \text{sign}(u_\lambda) = (a + K^* T_\gamma^2 (f - Ka))_\lambda \ .$$

This results in an explicit soft-shrinkage operation for u_λ

$$u_\lambda = S_\alpha((a + K^* T_\gamma^2 (f - Ka))_\lambda) \ .$$

The next proposition summarizes our findings; it is the specialization to our particular case of a more general theorem in [DDD03].

Proposition 3.2 *Suppose K is a linear bounded operator modeling the blur, with K maps $L_2(\Omega)$ to $L_2(\Omega)$ and $\|K^*K\| < 1$. Moreover, assume T_γ is defined as in* (3.5) *and the functional $\mathcal{F}_f^{sur}(\tilde{w}, u; a)$ is given by*

$$\mathcal{F}_f^{sur}(\tilde{w}_\gamma(f,u), u; a) = \mathcal{F}_f(\tilde{w}_\gamma(f,u), u) + \Phi(u; a) \ .$$

Then, for arbitrarily chosen $a \in L_2(\Omega)$, the functional $\mathcal{F}_f^{sur}(\tilde{w}_\gamma(f,u), u; a)$ has a unique minimizer in $L_2(\Omega)$. The minimizing element is given by

$$\tilde{u}_{\gamma,\alpha} = \mathbf{S}_\alpha(a + K^* T_\gamma^2 (f - Ka)) \ ,$$

where the operator $\mathbf{S}_\alpha$ is defined component-wise by

$$\mathbf{S}_\alpha(x) = \sum_\lambda S_\alpha(x_\lambda)\psi_\lambda \ .$$

The proof follows from [DDD03]. One can now define an iterative algorithm by repeated minimization of $\mathcal{F}_f^{sur}$:

$$u^0 \ \text{ arbitrary} \ ; \quad u^n = \arg\min_u \left(\mathcal{F}_f^{sur}(\tilde{w}_\gamma(f,u), u; u^{n-1})\right) \quad n = 1, 2, \ldots \tag{3.9}$$

The convergence result of [DDD03] can again be applied directly:

Theorem 3.1 *Suppose K is a linear bounded operator, with $\|K^*K\| < 1$, and that T_γ is defined as in* (3.5)*. Then the sequence of iterates*

$$u_{\gamma,\alpha}^n = \mathbf{S}_\alpha(u_{\gamma,\alpha}^{n-1} + K^* T_\gamma^2 (f - K u_{\gamma,\alpha}^{n-1})) \ , \quad n = 1, 2, \ldots \quad ,$$

with arbitrarily chosen $u^0 \in L_2(\Omega)$, converges in norm to a minimizer $\tilde{u}_{\gamma,\alpha}$ of the functional

$$\mathcal{F}_f(\tilde{w}_\gamma(f,u), u) = \|T_\gamma(f - Ku)\|_{L_2(\Omega)}^2 + 2\alpha |u|_{B_1^1(L_1(\Omega))} \ .$$

If $\mathcal{N}(T_\gamma K) = \{0\}$, then the minimizer $\tilde{u}_{\gamma,\alpha}$ is unique, and every sequence of iterates converges to $\tilde{u}_{\gamma,\alpha}$ in norm.

Combining the result of Theorem 3.1 and the representation for $\tilde{v}$ we summarize how the image can finally be decomposed in cartoon and oscillating components.

Corollary 3.1 *Assume that K is a linear bounded operator modeling the blur, with $\|K^*K\| < 1$. Moreover, if T_γ is defined as in (3.5) and if $\tilde{u}_{\gamma,\alpha}$ is the minimizing element of (3.7), obtained as a limit of $u^n_{\gamma,\alpha}$ (see Theorem 3.1), then the variational problem*

$$\inf_{(u,w)} \mathcal{F}_f(w,u), \text{ with } \mathcal{F}_f(w,u) = \|f - K(u+Tw)\|^2_{L_2(\Omega)} + \gamma\|w\|^2_{L_2(\Omega)} + 2\alpha|u|_{B^1_1(L_1(\Omega))}$$

is minimized by the class

$$(\tilde{u}_{\gamma,\alpha}, (T^*K^*KT + \gamma)^{-1}T^*K^*(f - K\tilde{u}_{\gamma,\alpha})) \ .$$

4 Refinements: using redundancy and adaptivity to reduce artifacts

The non-linear filtering rule of Proposition 3.1 gives explicit descriptions of $\tilde{v}$ and $\tilde{u}$ that are computed by fast discrete wavelet schemes. However, non-redundant filtering very often creates artifacts in terms of undesirable oscillations, which manifest themselves as ringing and edge blurring. Poor directional selectivity of traditional tensor product wavelet bases likewise cause artifacts. In this section we discuss various refinements on the basic algorithm that address this problem. In particular, we shall use redundant translation invariant schemes, complex wavelets, and additional edge dependent penalty weights.

4.1 Translation invariance by cycle–spinning

Assume that we are given an image with 2^M rows of 2^M pixels, where the gray value of each pixel gives an average of f on a square $2^{-M} \times 2^{-M}$, which we denote by f^M_k, with k a double index running through all the elements of $\{0,1,\ldots,2^M - 1\} \times \{0,1,\ldots,2^M-1\}$. A traditional wavelet transform then computes f^j_l, $d^{j,i}_l$ with $j_0 \le j \le M$, $i = 1,2,3$ and $l \in \{0,1,\ldots,2^j-1\} \times \{0,1,\ldots,2^j-1\}$ for each j, where the f^j_l stand for an average of f on mostly localized on (and indexed by) the squares $[l_1 2^{-j}, (l_1+1)2^{-j}] \times [l_2 2^{-j}, (l_2+1)2^{-j}]$, and the $d^{j,i}_l$ stand for the different species of wavelets (in two dimensions, there are three) in the tensor product multi–resolution analysis. Because the corresponding wavelet basis is not translation invariant, Coifman and Donoho proposed in [CD95] to recover translation invariance by averaging over the $2^{2(M+1-j_0)}$ translates of the wavelet basis; since many wavelets occur in more than one of these translated bases (in fact, each $\psi_{j,i,k}(x - 2^M n)$ in exactly $2^{2(j+1-j_0)}$) different bases), the average over all these bases uses only $(M+1-j_0)2^{2M}$ different basis functions (and not $2^{4(M+1-j_0)}$ = number of bases $\times$ number of elements in each basis). This approach is called *cycle–spinning*. Writing, with a slight abuse of notation, $\psi_{j,i,k+2^{j-M}n}$ for the translate $\psi_{j,i,k}(x - 2^M n)$, this average can then be written as

$$f^M = 2^{-2(M+1-j_0)} \sum_{l_1,l_2=0}^{2^M-1} \left\{ f^{j_0}_{l2^{-M+j_0}} \phi_{j_0,l2^{-M+j_0}} + \sum_{j=j_0}^{M-1} 2^{2(j-j_0)} \sum_{i=1}^{3} d^{j,i}_{l2^{-M+j}} \psi_{j,i,l2^{-M+j}} \right\} \ .$$

Carrying out our nonlinear filtering in each of the bases and averaging the result then corresponds to applying the corresponding nonlinear filtering on the (much smaller number of) coefficients in the last expression. This is the standard way to implement thresholding on cycle–spinned representations.

The resulting sequence space representation of the variational functional (3.3) has to be adapted to the redundant representation of f. To this end, we note that the Besov penalty term takes the form

$$|f|_{B_p^\beta(L_p)} \sim \left(\sum_{j \geq j_0, i, k} 2^{(js+2(j-M))} |\langle f, \tilde{\psi}_{j,i,k2^{j-M}} \rangle|^p \right)^{1/p} .$$

The norms $\|\cdot\|_{L_2}^2$ and $\|\cdot\|_{H^{-1}}^2$ change similarly. Consequently, we obtain the same minimization rule but with respect to a richer class of wavelet coefficients.

4.2 Directional sensitivity by frequency projections

It has been shown by several authers [Kin99, Sel01, FvSCB00] that if one treats positive and negative frequencies separately in the one–dimensional wavelet transform (resulting in complex wavelets), the directional selectivity of the corresponding two–dimensional multi–resolution analysis is improved. This can be done by applying the following orthogonal projections

$$\begin{aligned} \mathcal{P}^+ &: L_2 \to L_{2,+} = \{f \in L_2 : \text{ supp } \hat{f} \subseteq [0, \infty)\} \\ \mathcal{P}^- &: L_2 \to L_{2,-} = \{f \in L_2 : \text{ supp } \hat{f} \subseteq (-\infty, 0]\} . \end{aligned}$$

The projectors $\mathcal{P}^+$ and $\mathcal{P}^-$ may be either applied to f or to $\{\phi, \tilde{\phi}\}$ and $\{\psi, \tilde{\psi}\}$. In a discrete framework these projections have to be approximated. This has been done in different ways in the literature. In [Kin99, Sel01] Hilbert transform pairs of wavelets are used. In [FvSCB00] f is projected (approximately) by multiplying with shifted generator symbols in the frequency domain. We follow the second approach, i.e.

$$(P^+ f)^\wedge(\omega) := \hat{f}(\omega) H(\omega - \pi/2) \text{ and } (P^- f)^\wedge(\omega) := \hat{f}(\omega) H(\omega + \pi/2) ,$$

where f denotes the function to be analyzed and H is the low–pass filter for a conjugate quadrature mirror filter pair. One then has

$$\hat{f}(\omega) = (B^+ P^+ f)^\wedge(\omega) + (B^- P^- f)^\wedge(\omega) , \tag{4.1}$$

where the back–projections are given by

$$(B^+ f)^\wedge = \hat{f} \overline{H(\cdot - \pi/2)} \text{ and } (B^- f)^\wedge = \hat{f} \overline{H(\cdot + \pi/2)}$$

respectively. This technique provides us with a simple multiplication scheme in Fourier, or equivalently, a convolution scheme in time domain. In a separable two–dimensional framework the projections need to be carried out in each of the two frequency variables, resulting in four approximate projection operators P^{++}, P^{+-}, P^{-+}, P^{--}. Because f is real, we have

$$(P^{++} f)^\wedge(-\omega) = \overline{(P^{--} f)^\wedge(\omega)} \text{ and } (P^{+-} f)^\wedge(-\omega) = \overline{(P^{-+} f)^\wedge(\omega)} ,$$

so that the computation of $P^{-+}f$ and $P^{--}f$ can be omitted. Consequently, the modified variational functional takes the form

$$\begin{aligned}\mathcal{F}_f(u,v) &= 2\left(\|P^{++}(f-(u+v))\|_{L_2}^2 + \|P^{+-}(f-(u+v))\|_{L_2}^2\right) + \\ &\qquad 2\lambda\left(\|P^{++}v\|_{H^{-1}}^2 + \|P^{+-}v\|_{H^{-1}}^2\right) + 2\alpha|u|_{B^1_{1(L_1)}} \\ &\leq 2\left(\|P^{++}(f-(u+v))\|_{L_2}^2 + \|P^{+-}(f-(u+v))\|_{L_2}^2\right) + \\ &\qquad 2\lambda\left(\|P^{++}v\|_{H^{-1}}^2 + \|P^{+-}v\|_{H^{-1}}^2\right) + \\ &\qquad 4\alpha\left(|P^{++}u|_{B^1_{1(L_1)}} + |P^{+-}u|_{B^1_{1(L_1)}}\right) ,\end{aligned}$$

which can be minimized with respect to $\{P^{++}v, P^{++}u\}$ and $\{P^{+-}v, P^{+-}u\}$ separately. The projections are be complex–valued, so that the thresholding operator needs to be adapted. Parameterizing the wavelet coefficients by modulus and angle and minimizing yields the following filtering rules for the projections of $\tilde{v}_{\gamma,\alpha}$ and $\tilde{u}_{\gamma,\alpha}$ (where $\cdot\cdot$ stands for any combination of $+$, $-$)

$$P^{\cdot\cdot}\tilde{v}_{\gamma,\alpha} = \sum_{\lambda\in J_{j_0}} (1+\gamma 2^{-2|\lambda|})^{-1}\left[P^{\cdot\cdot}f_\lambda - S_{\alpha(2^{2|\lambda|}+\gamma)/\gamma}(|P^{\cdot\cdot}f_\lambda|)e^{i\omega(P^{\cdot\cdot}f)}\right]\psi_\lambda$$

and

$$P^{\cdot\cdot}\tilde{u}_{\gamma,\alpha} = \sum_{k\in I_{j_0}} \langle P^{\cdot\cdot}f, \tilde{\phi}_{j_0,k}\rangle\phi_{j_0,k} + \sum_{\lambda\in J_{j_0}} (1+\gamma 2^{-2|\lambda|})^{-1} S_{\alpha(2^{2|\lambda|}+\gamma)/\gamma}(|P^{\cdot\cdot}f_\lambda|)e^{i\omega(P^{\cdot\cdot}f)}\psi_\lambda \ .$$

Finally, we have to apply the back-projections to obtain the minimizing functions

$$\tilde{v}^{BP}_{\gamma,\alpha} = B^{++}P^{++}\tilde{v}_{\gamma,\alpha} + B^{--}\overline{P^{++}\tilde{v}_{\gamma,\alpha}} + B^{+-}P^{+-}\tilde{v}_{\gamma,\alpha} + B^{-+}\overline{P^{+-}\tilde{v}_{\gamma,\alpha}}$$

and

$$\tilde{u}^{BP}_{\gamma,\alpha} = B^{++}P^{++}\tilde{u}_{\gamma,\alpha} + B^{--}\overline{P^{++}\tilde{u}_{\gamma,\alpha}} + B^{+-}P^{+-}\tilde{u}_{\gamma,\alpha} + B^{-+}\overline{P^{+-}\tilde{u}_{\gamma,\alpha}} \ .$$

4.3 Weighted penalty functions

In order to improve the capability of preserving edges we additionally introduce a positive weight sequence w_λ in the H^{-1} penalty term. Consequently, we aim at minimizing a slightly modified sequence space functional

$$\sum_{\lambda\in J}\left(|f_\lambda - (u_\lambda+v_\lambda)|^2 + \gamma 2^{-2|\lambda|}w_\lambda|v_\lambda|^2 + 2\alpha|u_\lambda|\cdot 1_{\{\lambda\in J_{j_0}\}}\right) \ . \tag{4.2}$$

The resulting texture and cartoon components take the form

$$\tilde{v}^{w}_{\gamma,\alpha} = \sum_{\lambda\in J_{j_0}} (1+\gamma w_\lambda 2^{-2|\lambda|})^{-1}\left[f_\lambda - S_{\alpha(2^{2|\lambda|}+\gamma w_\lambda)/\gamma w_\lambda}(f_\lambda)\right]\psi_\lambda$$

and

$$\tilde{u}^w_{\gamma,\alpha} = \sum_{k\in I_{j_0}} \langle f, \tilde{\phi}_{j_0,k}\rangle \phi_{j_0,k} + \sum_{\lambda\in J_{j_0}} S_{\alpha(2^{2|\lambda|}+\gamma w_\lambda)/\gamma w_\lambda}(f_\lambda)\psi_\lambda \ .$$

The main goal is to introduce a control parameter that depends on the local structure of f. The local penalty weight w_λ should be large in the presence of an edge and small otherwise; the result of this weighting is to enhance the sensitivity of u near edges. In order to do this, we must first localize the edges, which we do by a procedure similar to an edge detection algorithm in [MZ92]. This scheme rests on the analysis of the cycle-spinned wavelet coefficients f_λ at or near the same location but at different scales. We expect that the f_λ belonging to fine decomposition scales contain informations of edges (well localized) as well as oscillating components. Texture oscillating components typically show up in fine scales only; edges on the other hand leave a signature of larger wavelet coefficients through a wider range of scales. We thus apply the following not very sophisticated edge detector. Suppose that $f \in V_M$ and j_e denotes some 'critical' scale, then for a certain range of scales $|\lambda| = |(i,j,k)| = j \in \{j_0, \ldots, j_1 - j_e - 2, j_1 - j_e - 1\}$ we mark all positions k where $|f_\lambda|$ is larger than a level dependent threshold parameter t_j. Here the value t_j is chosen proportional to the mean value of all wavelet coefficients of level j. We say that $|f_\lambda|$ represents an edge if k was marked for all $j \in \{j_0, \ldots, j_1 - j_e - 2, j_1 - j_e - 1\}$. Finally, we adaptively choose the penalty sequence by setting

$$w_\lambda = \begin{cases} \Theta_\lambda & \text{if } j \in \{M-1, \ldots, j_1 - j_e\} \text{ and } k \text{ was marked as an edge ,} \\ \vartheta_\lambda & \text{otherwise ,} \end{cases}$$

where ϑ_λ is close to one and Θ_λ is much larger in order to penalize the corresponding v_λ's.

5 Numerical experiments

In this section, we present some numerical experiments obtained with our wavelet–based schemes.

We start with the case where K is the identity operator. In order to show how the nonlinear (redundant) wavelet scheme acts on piecewise constant functions we decompose a geometric image (representing cartoon components only) with sharp contours, see Figure 1. We observe that $\tilde{u}$ represents the cartoon part very well. The texture component $\tilde{v}$ (plus a constant for illustration purposes) contains only some very weak contour structures. Next, in Figure 2 we demonstrate the performance of the algorithm successively incorporating translation invariance and local penalty weights. The upper row of images shows the decomposition where the non-redundant Haar basis was used. Such a nonlinear filtering leads to undesired blocking artifacts. An improvement is shown in the middle row where we have used a translation invariant representation by cycle spinning. We may clearly observe that cycle spinning cause edge blurring. This can be reduced by involving additional local dependent penalty weights as described in Section 4.3, see lower row in Figure 2. The next experiment is done on a fabric image, see Figure 3. But in contrast to the examples before, we present here the use of frequency projection as introduced in Section 4.2. The numerical result shows convincingly that the texture component can be also

Figure 1: From left to right: initial geometric image f, $\tilde{u}$, $\tilde{v} + 150$, computed with Db3 in the translation invariant setting, $\alpha = 0.5$, $\gamma = 0.01$.

well separated from the cartoon part. In order to compare the performance with the Vese–Osher TV model and with the Vese–Solé–Osher H^{-1} model we apply our scheme to a woman image (the same that was used in [OV02, OSV02]). We obtain very similar results as obtained with the TV model proposed in [OV02]. Compared with the results obtained with the H^{-1} model proposed in [OSV02] we observe that our reconstruction of the texture component contains much less cartoon information.

We end this section with presenting an experiment where K is not the identity operator. In our particular case K is a convolution operator with Gaussian kernel. The implementation is simply done in Fourier space. The upper row in Figure 5 shows the original f and the blurred image Kf. The lower row visualizes the results: the cartoon component $\tilde{u}$, the texture component $\tilde{v}$, and the sum of both $\tilde{u}+\tilde{v}$. One may clearly see that the deblurred image $\tilde{u} + \tilde{v}$ contains (after a small number of iterations) more small scale details than Kf. This definitely shows the capabilities of the proposed iterative deblurring scheme (3.9).

Acknowledgements

The authors would like to thank L. Vese, S. Osher, C. DeMol and M. Defrise for very interesting and stimulating discussions. I.D. gratefully acknowledges support by Air Force grant F49620-01-1-0099, and by NSF grants DMS-0219233 and DMS-0245566. G.T. gratefully acknowledges support by DAAD grants as well as by DFG grant Te 354/1-2, and moreover, he especially thanks the PACM and the ULB for their hospitality during his stays in Princeton and Brussels.

References

[CD95] R.R. Coifman and D. Donoho. Translation–invariant de–noising. in *Wavelets and Statistics, A. Antoniadis and G. Oppenheim,* eds., Springer–Verlag, New York, pages 125–150, 1995.

[CDF92] A. Cohen, I. Daubechies, and J.-C. Feauveau. Biorthogonal bases of compactly supported wavelets. *Comm. Pure Appl. Math.*, 45:485–560, 1992.

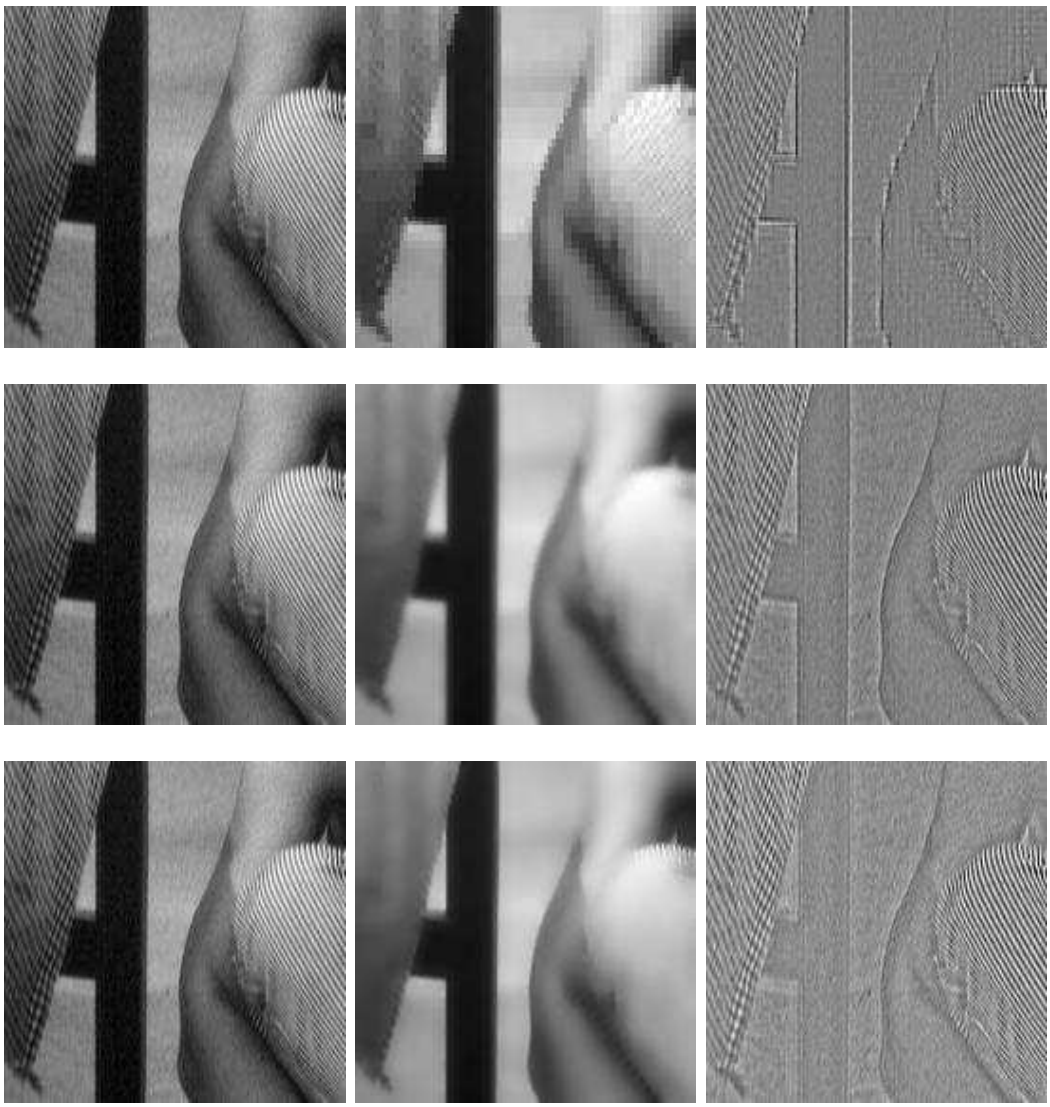

Figure 2: Top: non-redundant filtering, middle: with edge enhancement, bottom: without edge enhancement; From left to right: initial image f, $\tilde{u}$, $\tilde{v} + 150$, $\alpha = 0.5$, $\gamma = 0.0001$, computed with Db1 and critical scale $j_e = -3$.

[CDPX99] A. Cohen, R. DeVore, P. Petrushev, and H. Xu. Nonlinear Approximation and the Space $BV(\mathbb{R}^2)$. *American Journal of Mathematics*, (121):587–628, 1999.

[Dah96] W. Dahmen. Stability of multiscale transformations. *The Journal of Fourier Analysis and Applications*, 2:341–361, 1996.

[Dau92] I. Daubechies. *Ten Lectures on Wavelets*. SIAM, Philadelphia, 1992.

[Dau93] I. Daubechies. Wavelet transforms and orthonormal wavelet bases. *Proceedings of Symposia in Applied Mathematics*, (47), 1993.

[DD03a] M. Defrise and C. DeMol. Inverse imaging with mixed penalties. *Conference proceedings*, 2003.

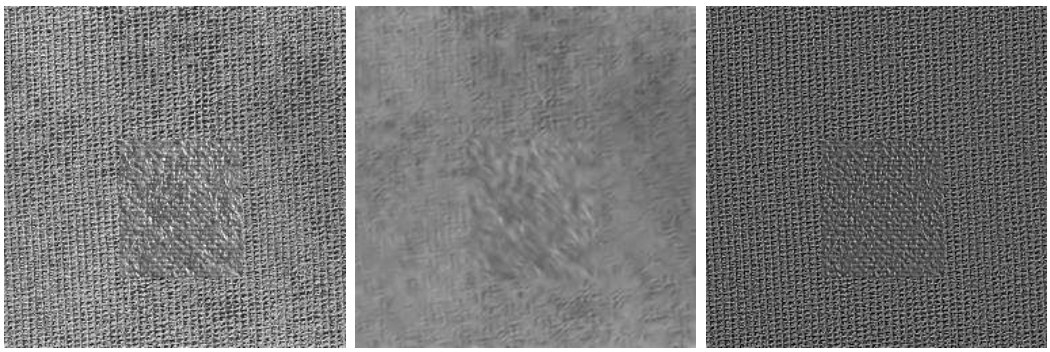

Figure 3: From left to right: initial fabric image f, $\tilde{u}$, $\tilde{v} + 150$, computed with Db4 incorporating frequency projections, $\alpha = 0.8$, $\gamma = 0.002$.

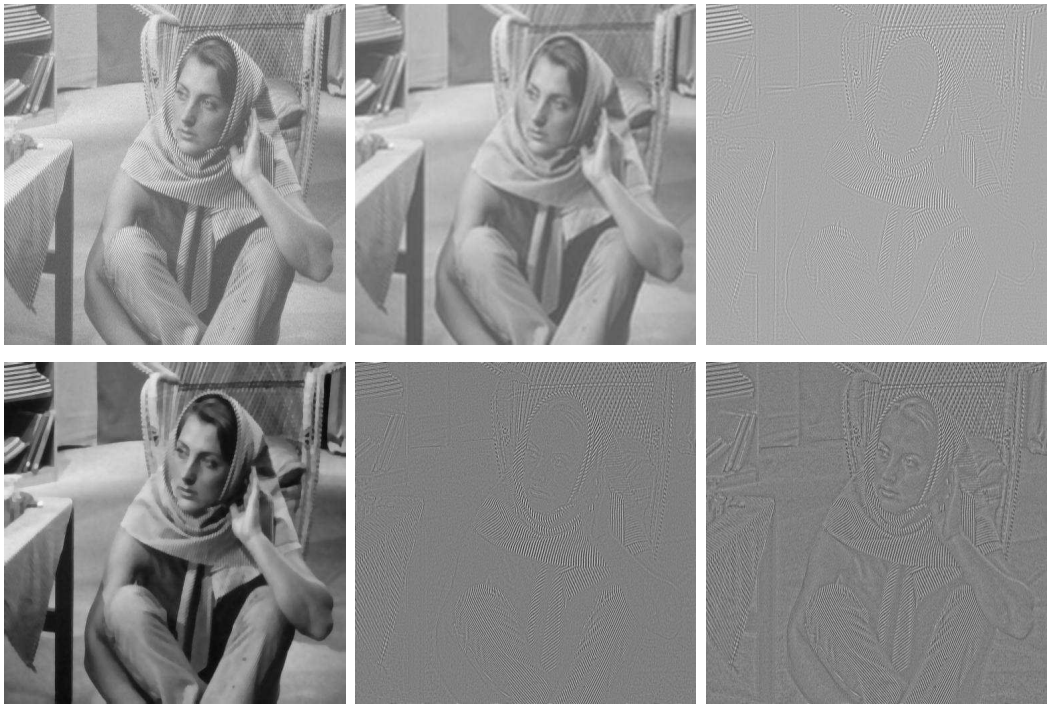

Figure 4: Top from left to right: initial woman image f, $\tilde{u}$ and $\tilde{v} + 150$, computed with Db10 incorporating frequency projections, $\alpha = 0.5$, $\gamma = 0.002$; bottom from left to right: u and v obtained by the Vese–Osher TV model and the v component obtained by the Vese–Solé–Osher H^{-1} model (the scale of gray values is slightly different) .

[DD03b] M. Defrise and C. DeMol. Linear inverse problems with mixed smoothness and sparsity constraints. *Preprint*, 2003.

[DDD03] I. Daubechies, M. Defrise, and C. DeMol. An iterative thresholding algorithm for linear inverse problems with a sparsity constraint. *Preprint*, 2003.

[DeV98] R. DeVore. Nonlinear Approximation. *Acta Numerica*, 7:51–150, 1998.

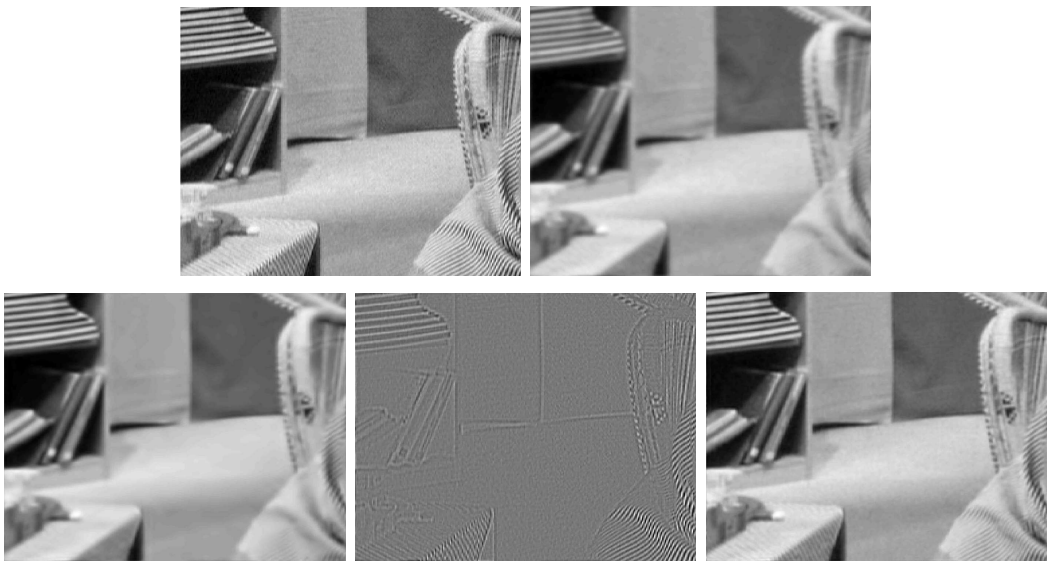

Figure 5: Top from left to right: initial image f, blurred image Kf; bottom from left to right: deblurred $\tilde{u}$, deblurred $\tilde{v} + 150$, deblurred $\tilde{u} + \tilde{v}$, computed with Db3 using the iterative approach, $\alpha = 0.2$, $\gamma = 0.001$.

[DJP88] R. DeVore, B. Jawerth, and V. Popov. Interpolation of besov spaces. *Trans. Math. Soc.*, 305:397–414, 1988.

[DJP92] R. DeVore, B. Jawerth, and V. Popov. Compression of wavelet decompositions. *Amer. J. Math.*, 114:737–785, 1992.

[DT04] I. Daubechies and G. Teschke. Wavelet based image decomposition by variational functional. *to appear in SPIE proceedings*, 2004.

[FJ90] M. Frazier and B. Jawerth. A discrete transform and decompositions of distribution spaces. *J. of Functional Anal.*, 93:34–170, 1990.

[FvSCB00] F. C. A. Fernandes, R. v. Spaendonck, M. J. Coates, and S. Burrus. Directional Complex-Wavelet Processing. *Proceedings of Society of Photo-Optical Instrumental Engineers—SPIE2000, Wavelet Applications in Signal Processing VIII,* San Diego., 2000.

[Kin99] N. Kinsbury. Image processing with complex wavelets. *Phil. Trans. R. Soc. Lond.*, Sept. 1999.

[Mey02] Y. Meyer. Oscillating Patterns in Image Processing and Nonlinear Evolution Equations. *University Lecture Series Volume 22, AMS*, 2002.

[MZ92] S. Mallat and S. Zhong. Characterization of Signals from Multiscale Edges. *IEEE Transactions on Pattern Analysis and Machine Intelligence*, 14(7):710–732, July 1992.

[OSV02] S. Osher, A. Sole, and L. Vese. Image decomposition and restoration using total variation minimization and the H^{-1} norm. Technical Report 02-57, University of California Los Angeles C.A.M., 2002.

[OV02] S. Osher and L. Vese. Modeling textures with total variation minimization and oscillating patterns in image processing. Technical Report 02-19, University of California Los Angeles C.A.M., 2002.

[ROF92] L. Rudin, S. Osher, and E. Fatemi. Nonlinear total variations based noise removal algorithms. *Physica D*, 60:259–268, 1992.

[Sel01] I. W. Selesnick. Hilbert transform pairs of wavelet bases. *IEEE Signal Processing Letters*, 8(6):170–173, June 2001.

[Tri78] H. Triebel. *Interpolation Theory, Function Spaces, Differential Operators*. Verlag der Wissenschaften, Berlin, 1978.

Berichte aus der Technomathematik ISSN 1435-7968

http://www.math.uni-bremen.de/zetem/berichte.html

— Vertrieb durch den Autor —

Reports **Stand: 23. April 2004**

98–01. Peter Benner, Heike Faßbender:
An Implicitly Restarted Symplectic Lanczos Method for the Symplectic Eigenvalue Problem, Juli 1998.

98–02. Heike Faßbender:
Sliding Window Schemes for Discrete Least-Squares Approximation by Trigonometric Polynomials, Juli 1998.

98–03. Peter Benner, Maribel Castillo, Enrique S. Quintana-Ortí:
Parallel Partial Stabilizing Algorithms for Large Linear Control Systems, Juli 1998.

98–04. Peter Benner:
Computational Methods for Linear–Quadratic Optimization, August 1998.

98–05. Peter Benner, Ralph Byers, Enrique S. Quintana-Ortí, Gregorio Quintana-Ortí:
Solving Algebraic Riccati Equations on Parallel Computers Using Newton's Method with Exact Line Search, August 1998.

98–06. Lars Grüne, Fabian Wirth:
On the rate of convergence of infinite horizon discounted optimal value functions, November 1998.

98–07. Peter Benner, Volker Mehrmann, Hongguo Xu:
A Note on the Numerical Solution of Complex Hamiltonian and Skew-Hamiltonian Eigenvalue Problems, November 1998.

98–08. Eberhard Bänsch, Burkhard Höhn:
Numerical simulation of a silicon floating zone with a free capillary surface, Dezember 1998.

99–01. Heike Faßbender:
The Parameterized SR Algorithm for Symplectic (Butterfly) Matrices, Februar 1999.

99–02. Heike Faßbender:
Error Analysis of the symplectic Lanczos Method for the symplectic Eigenvalue Problem, März 1999.

99–03. Eberhard Bänsch, Alfred Schmidt:
Simulation of dendritic crystal growth with thermal convection, März 1999.

99–04. Eberhard Bänsch:
Finite element discretization of the Navier-Stokes equations with a free capillary surface, März 1999.

99–05. Peter Benner:
Mathematik in der Berufspraxis, Juli 1999.

99–06. Andrew D.B. Paice, Fabian R. Wirth:
Robustness of nonlinear systems and their domains of attraction, August 1999.

99–07. Peter Benner, Enrique S. Quintana-Ortí, Gregorio Quintana-Ortí:
Balanced Truncation Model Reduction of Large-Scale Dense Systems on Parallel Computers, September 1999.

99–08. Ronald Stöver:
Collocation methods for solving linear differential-algebraic boundary value problems, September 1999.

99–09. Huseyin Akcay:
Modelling with Orthonormal Basis Functions, September 1999.

99–10. Heike Faßbender, D. Steven Mackey, Niloufer Mackey:
Hamilton and Jacobi come full circle: Jacobi algorithms for structured Hamiltonian eigenproblems, Oktober 1999.

99–11. Peter Benner, Vincente Hernández, Antonio Pastor:
On the Kleinman Iteration for Nonstabilizable System, Oktober 1999.

99–12. Peter Benner, Heike Faßbender:
A Hybrid Method for the Numerical Solution of Discrete-Time Algebraic Riccati Equations, November 1999.

99–13. Peter Benner, Enrique S. Quintana-Ortí, Gregorio Quintana-Ortí:
Numerical Solution of Schur Stable Linear Matrix Equations on Multicomputers, November 1999.

99–14. Eberhard Bänsch, Karol Mikula:
Adaptivity in 3D Image Processing, Dezember 1999.

00–01. Peter Benner, Volker Mehrmann, Hongguo Xu:
Perturbation Analysis for the Eigenvalue Problem of a Formal Product of Matrices, Januar 2000.

00–02. Ziping Huang:
Finite Element Method for Mixed Problems with Penalty, Januar 2000.

00–03. Gianfrancesco Martinico:
Recursive mesh refinement in 3D, Februar 2000.

00–04. Eberhard Bänsch, Christoph Egbers, Oliver Meincke, Nicoleta Scurtu:
Taylor-Couette System with Asymmetric Boundary Conditions, Februar 2000.

00–05. Peter Benner:
Symplectic Balancing of Hamiltonian Matrices, Februar 2000.

00–06. Fabio Camilli, Lars Grüne, Fabian Wirth:
A regularization of Zubov's equation for robust domains of attraction, März 2000.

00–07. Michael Wolff, Eberhard Bänsch, Michael Böhm, Dominic Davis:
Modellierung der Abkühlung von Stahlbrammen, März 2000.

00–08. Stephan Dahlke, Peter Maaß, Gerd Teschke:
Interpolating Scaling Functions with Duals, April 2000.

00–09. Jochen Behrens, Fabian Wirth:
A globalization procedure for locally stabilizing controllers, Mai 2000.

00–10. Peter Maaß, Gerd Teschke, Werner Willmann, Günter Wollmann:
Detection and Classification of Material Attributes – A Practical Application of Wavelet Analysis, Mai 2000.

00–11. Stefan Boschert, Alfred Schmidt, Kunibert G. Siebert, Eberhard Bänsch, Klaus-Werner Benz, Gerhard Dziuk, Thomas Kaiser:
Simulation of Industrial Crystal Growth by the Vertical Bridgman Method, Mai 2000.

00–12. Volker Lehmann, Gerd Teschke:
Wavelet Based Methods for Improved Wind Profiler Signal Processing, Mai 2000.

00–13. Stephan Dahlke, Peter Maass:
A Note on Interpolating Scaling Functions, August 2000.

00–14. Ronny Ramlau, Rolf Clackdoyle, Frédéric Noo, Girish Bal:
Accurate Attenuation Correction in SPECT Imaging using Optimization of Bilinear Functions and Assuming an Unknown Spatially-Varying Attenuation Distribution, September 2000.

00–15. Peter Kunkel, Ronald Stöver:
Symmetric collocation methods for linear differential-algebraic boundary value problems, September 2000.

00–16. Fabian Wirth:
The generalized spectral radius and extremal norms, Oktober 2000.

00–17. Frank Stenger, Ahmad Reza Naghsh-Nilchi, Jenny Niebsch, Ronny Ramlau:
A unified approach to the approximate solution of PDE, November 2000.

00–18. Peter Benner, Enrique S. Quintana-Ortí, Gregorio Quintana-Ortí:
Parallel algorithms for model reduction of discrete–time systems, Dezember 2000.

00–19. Ronny Ramlau:
A steepest descent algorithm for the global minimization of Tikhonov–Phillips functional, Dezember 2000.

01–01. Efficient methods in hyperthermia treatment planning:
Torsten Köhler, Peter Maass, Peter Wust, Martin Seebass, Januar 2001.

01–02. Parallel Algorithms for LQ Optimal Control of Discrete-Time Periodic Linear Systems:
Peter Benner, Ralph Byers, Rafael Mayo, Enrique S. Quintana-Ortí, Vicente Hernández, Februar 2001.

01–03. Peter Benner, Enrique S. Quintana-Ortí, Gregorio Quintana-Ortí:
Efficient Numerical Algorithms for Balanced Stochastic Truncation, März 2001.

01–04. Peter Benner, Maribel Castillo, Enrique S. Quintana-Ortí:
Partial Stabilization of Large-Scale Discrete-Time Linear Control Systems, März 2001.

01–05. Stephan Dahlke:
Besov Regularity for Edge Singularities in Polyhedral Domains, Mai 2001.

01–06. Fabian Wirth:
A linearization principle for robustness with respect to time-varying perturbations, Mai 2001.

01–07. Stephan Dahlke, Wolfgang Dahmen, Karsten Urban:
Adaptive Wavelet Methods for Saddle Point Problems - Optimal Convergence Rates, Juli 2001.

01–08. Ronny Ramlau:
Morozov's Discrepancy Principle for Tikhonov regularization of nonlinear operators, Juli 2001.

01–09. Michael Wolff:
Einführung des Drucks für die instationären Stokes–Gleichungen mittels der Methode von Kaplan, Juli 2001.

01–10. Stephan Dahlke, Peter Maaß, Gerd Teschke:
Reconstruction of Reflectivity Desities by Wavelet Transforms, August 2001.

01–11. Stephan Dahlke:
Besov Regularity for the Neumann Problem, August 2001.

01–12. Bernard Haasdonk, Mario Ohlberger, Martin Rumpf, Alfred Schmidt, Kunibert G. Siebert:
h–p–Multiresolution Visualization of Adaptive Finite Element Simulations, Oktober 2001.

01–13. Stephan Dahlke, Gabriele Steidl, Gerd Teschke:
Coorbit Spaces and Banach Frames on Homogeneous Spaces with Applications to Analyzing Functions on Spheres, August 2001.

02–01. Michael Wolff, Michael Böhm:
Zur Modellierung der Thermoelasto-Plastizität mit Phasenumwandlungen bei Stählen sowie der Umwandlungsplastizität, Februar 2002.

02–02. Stephan Dahlke, Peter Maaß:
An Outline of Adaptive Wavelet Galerkin Methods for Tikhonov Regularization of Inverse Parabolic Problems, April 2002.

02–03. Alfred Schmidt:
A Multi-Mesh Finite Element Method for Phase Field Simulations, April 2002.

02–04. Sergey N. Dachkovski, Michael Böhm:
A Note on Finite Thermoplasticity with Phase Changes, Juli 2002.

02–05. Michael Wolff, Michael Böhm:
Phasenumwandlungen und Umwandlungsplastizität bei Stählen im Konzept der Thermoelasto-Plastizität, Juli 2002.

02–06. Gerd Teschke:
Construction of Generalized Uncertainty Principles and Wavelets in Anisotropic Sobolev Spaces, August 2002.

02–07. Ronny Ramlau:
TIGRA – an iterative algorithm for regularizing nonlinear ill–posed problems, August 2002.

02–08. Michael Lukaschewitsch, Peter Maaß, Michael Pidcock:
Tikhonov regularization for Electrical Impedance Tomography on unbounded domains, Oktober 2002.

02–09. Volker Dicken, Peter Maaß, Ingo Menz, Jenny Niebsch, Ronny Ramlau:
Inverse Unwuchtidentifikation an Flugtriebwerken mit Quetschöldämpfern, Oktober 2002.

02–10. Torsten Köhler, Peter Maaß, Jan Kalden:
Time-series forecasting for total volume data and charge back data, November 2002.

02–11. Angelika Bunse-Gerstner:
A Short Introduction to Iterative Methods for Large Linear Systems, November 2002.

02–12. Peter Kunkel, Volker Mehrmann, Ronald Stöver:
Symmetric Collocation for Unstructured Nonlinear Differential-Algebraic Equations of Arbitrary Index, November 2002.

02–13. Michael Wolff:
Ringvorlesung: Distortion Engineering 2
Kontinuumsmechanische Modellierung des Materialverhaltens von Stahl unter Berücksichtigung von Phasenumwandlungen, Dezember 2002.

02–14. Michael Böhm, Martin Hunkel, Alfred Schmidt, Michael Wolff:
Evaluation of various phase-transition models for 100Cr6 for application in commercial FEM programs, Dezember 2002.

03–01. Michael Wolff, Michael Böhm, Serguei Dachkovski:
Volumenanteile versus Massenanteile - der Dilatometerversuch aus der Sicht der Kontinuumsmechanik, Januar 2003.

03–02. Daniel Kessler, Ricardo H. Nochetto, Alfred Schmidt:
A posteriori error control for the Allen-Cahn Problem: circumventing Gronwall's inequality, März 2003.

03–03. Michael Böhm, Jörg Kropp, Adrian Muntean:
On a Prediction Model for Concrete Carbonation based on Moving Interfaces - Interface concentrated Reactions, April 2003.

03–04. Michael Böhm, Jörg Kropp, Adrian Muntean:
A Two-Reaction-Zones Moving-Interface Model for Predicting $Ca(OH)_2$ Carbonation in Concrete, April 2003.

03–05. Vladimir L. Kharitonov, Diederich Hinrichsen:
Exponential estimates for time delay systems, May 2003.

03–06. Michael Wolff, Michael Böhm, Serguei Dachkovski, Günther Löwisch:
Zur makroskopischen Modellierung von spannungsabhängigem Umwandlungsverhalten und Umwandlungsplastizität bei Stählen und ihrer experimentellen Untersuchung in einfachen Versuchen, Juli 2003.

03–07. Serguei Dachkovski, Michael Böhm, Alfred Schmidt, Michael Wolff:
Comparison of several kinetic equations for pearlite transformation in 100Cr6 steel,
Juli 2003.

03–08. Volker Dicken, Peter Maass, Ingo Menz, Jenny Niebsch, Ronny Ramlau:
Nonlinear Inverse Unbalance Reconstruction in Rotor dynamics,
Juli 2003.

03–09. Michael Böhm, Serguei Dachkovski, Martin Hunkel, Thomas Lübben, Michael Wolff:
Übersicht über einige makroskopische Modelle für Phasenumwandlungen im Stahl,
Juli 2003.

03–10. Michael Wolff, Friedhelm Frerichs, Bettina Suhr:
Vorstudie für einen Bauteilversuch zur Umwandlungsplastizität bei der perlitischen Umwandlung des Stahls 100 Cr6,
August 2003.

03–11. Michael Wolff, Bettina Suhr:
Zum Vergleich von Massen- und Volumenanteilen bei der perlitischen Umwandlung der Stähle 100Cr6 und C80,
September 2003.

03–12. Rike Grotmaack, Adrian Muntean:
Stabilitätsanalyse eines Moving-Boundary-Modells der beschleunigten Karbonatisierung von Portlandzementen,
September 2003.

03–13. Alfred Schmidt, Michael Wolff, Michael Böhm:
Numerische Untersuchungen für ein Modell des Materialverhaltens mit Umwandlungsplastizität und Phasenumwandlungen beim Stahl 100Cr6 (Teil 1),
September 2003.

04–01. Liliana Cruz Martin, Gerd Teschke:
A new method to reconstruct radar reflectivities and Doppler information,
Januar 2004.

04–02. Ingrid Daubechies, Gerd Teschke:
Wavelet based image decomposition by variational functionals,
Januar 2004.

04–03. N. Guglielmi, F. Wirth, M. Zennaro:
Complex polytope extremality results for families of matrices,
März 2004.

04–04. I. Daubechies, G. Teschke:
Variational image restoration by means of wavelets: simultaneous decomposition, deblurring and denoising,
April 2004.